Colloids and Surfaces A: Physicochemical and Engineering Aspects 700 (2024) 134694

Contents lists available at ScienceDirect

Colloids and Surfaces A: Physicochemical and Engineering Aspects

journal homepage: www.elsevier.com/locate/colsurfa

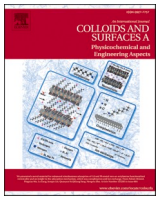

Ionic strength effect on the structure and dynamics of colloidal dispersions with weak attractive interactions

Claude Oelschlaeger *, Bruna Regina Maciel, Louise Ratel, Marc Müller, Norbert Willenbacher

Karlsruhe Institute of Technology (KIT), Institute for Mechanical Process Engineering and Mechanics, Karlsruhe 76131, Germany

HIGHLIGHTS

- Rheology and microrheology of colloidal dispersions with attractive interactions.
- Ionic strength effect on phase behavior, structure and flow properties.
- Increasing ionic strength reduces the effective particle volume fraction.
- Increasing ionic strength shifts the concentrations of phase transitions to lower polymer concentrations.

GRAPHICAL ABSTRACT

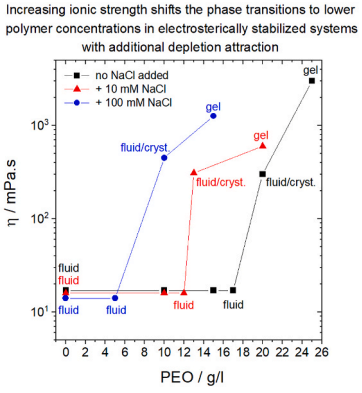

ARTICLE INFO

Keywords:
Colloidal dispersions
Ionic strength
Phase transition
MPT Microrheology
Rheology

ABSTRACT

We present a macro- and microrheological study of the effect of ionic strength on the phase behavior, structure and flow properties of colloidal dispersions stabilized by short-range repulsive interactions inferred via co-polymerization of weak acid groups. We investigated the impact of ionic strength, by varying the concentration of natrium chloride (NaCl), on dispersions with only repulsive interactions, but also when additional attractive depletion forces are present due to added non-absorbent polymer, namely polyethyleneoxide (PEO). For dispersions with only repulsive electrosteric interactions, at low particle volume fractions ($\phi < 0.4$), increasing ionic strength hardly affects the relative viscosity whereas at higher particle volume fractions, a decrease in viscosity is observed due to a reduced range of electrosteric repulsion between particles, corresponding to a reduction of the effective particle volume fraction ϕ_{eff}. For dispersions including attractive interactions, at volume fractions $\phi = 0.45$ below the hard sphere freezing point (ϕ_c=0.5), independently of the ionic strength, the bulk viscosity increases monotonically with increasing PEO concentration due to the transition from a fluid to a fluid/crystalline and finally to a gel state. However, the increase in ionic strength shifts the concentrations of both phase transitions to lower polymer concentrations, indicating that in presence of salt a weaker attraction is required to induce these transitions. At ϕ=0.52, just above ϕ_c, for dispersions without added salt, broadening of the fluid-crystalline coexistence regime, due to added PEO, results in a viscosity minimum corresponding to different size and packing density of the crystalline regions as observed earlier in Weis et al. [1].

* Corresponding author:.
E-mail address: claude.oelschlaeger@kit.edu (C. Oelschlaeger).

https://doi.org/10.1016/j.colsurfa.2024.134694
Received 9 April 2024; Received in revised form 4 June 2024; Accepted 2 July 2024
Available online 8 July 2024

When salt is added, the initial state for dispersions without PEO is a fluid state due to the reduction of ϕ_{eff} and the addition of a small amount of PEO leads to an increase in bulk viscosity due to the formation of large crystals for dispersions containing 10 mM NaCl and a network of small, dense crystals of size ≈10 μm when 100 mM NaCl is added. At ϕ=0.54, a result similar to ϕ=0.52 is obtained for dispersions without added salt, whereas in presence of salt, we find that the fluid/crystalline coexistence regime narrows down as the range of electrosteric repulsion decreases and the addition of PEO results in gel formation and gels become more uniform with increasing attraction strength. These investigations demonstrate how superimposed short range electrosteric repulsion and weak depletion attraction affect microstructure and flow behavior of colloidal dispersions.

1. Introduction

The understanding of the phase behavior of colloidal dispersions is a global research topic and is of utmost im- portance for several reasons. First, colloidal dispersions serve as model systems for fundamental physical phenomena studies like crystallization, gelation and glass formation at conveniently accessible time- and length scales [2–4]. Second, from a technical point of view, knowledge of the phase behavior under different conditions helps to optimize manufacturing processes, ensuring efficient production and product quality as well as cost reduction. It also allows the development and formulation of stable products with desired properties such as texture, consistency and shelf-life. Finally, colloidal dispersions are widely used in fabrication of nanostructured materials in emerging innovative fields of application, e. g. photonic crystals [5,6] but also in well-established commodity products like pharmaceuticals, food, coatings and adhesives [7,8]. A key technological challenge is to control their flow properties in order to meet the manifold challenges during processing and application. Numerous experimental [1,9–11] as well as theoretical studies and numerical simulations [12,13] have already been carried out for the understanding of the phase behavior. Colloidal crystals may be destroyed in strong shear flow but on the other hand in microfluidic devices preferential crystallization at the channel walls may result in cessation of flow [14].

In many studies [15–18] but in particular, in the study of Weis et al. [1], authors showed that phase behavior, structure and dynamics of dispersions of colloidal particles with short-range repulsive interactions can be modified via introduction of weak attractive interactions by adding non-absorbing polymers to the continuous phase. They found that at particle volume fractions below the hard sphere freezing point ($\phi_c < 0.5$), introducing attractive interaction resulted into a transition from a homogeneous fluid state to a fluid/crystalline coexistence region and with further increase of attraction strength to a gel-state. Macroscopically, this change in phase behavior showed up as a steady increase of low-shear viscosity. Additionally, for the first time, microstructural and local mechanical properties of these dispersions were accurately characterized in the different phase states using the Multiple Particle Tracking (MPT) based microrheology technique. MPT enabled direct imaging of formed micron-sized crystals and the determination of local rheological properties, namely the shear modulus of the crystals and the fluid viscosity using image Overlay and Voronoi triangulation. A completely different behavior was observed with the addition of non-adsorbing polymer in the fluid/crystalline coexistence region ($0.5 < \phi_c < 0.55$). In that case, at low polymer concentration, a first decrease of the low-shear viscosity was observed followed by a viscosity increase with increasing attraction strength. This behavior could be attributed to a change in the size and density of the formed crystals. Furthermore, the shear modulus of the micron-sized crystals could be directly determined using MPT and its variation with attraction strength was investigated systematically.

Based on this previous work applied to “salt-free” aqueous colloidal dispersions, the aim of this study is to investigate how these different transition phenomena are affected by ionic strength, since the colloidal polymer particles used in this study included co-polymerized weak acid groups resulting in the formation of a “hairy surface layer” upon neutralization and hence gave rise to a short range electrosteric repulsion [1,10]. A detailed description how ionic strength affects the electrosteric stabilization of colloidal dispersions is reported in Fritz et al. [19]. In this latter study, it was shown, that the shrinkage of the hairy surface layer upon addition of salt is the relevant mechanism controlling stability and flow of electrosterically stabilized colloidal dispersions. Increasing the ionic strength results in a screening of electrostatic repulsion among charged groups within the hairy surface layer which finally leads to a shrinkage of the layer and hence to a weaker steric repulsion. Other studies [20–22], in particular dynamic light scattering experiments performed on similar systems have confirmed the validity of this mechanism, namely that the colloidal stability is controlled by the variation of the surface layer thickness which depends on ionic strength. Not only the stability of these systems but also their flow properties are affected by ionic strength. It is well established that ionic strength impacts the volume fraction dependence of dispersion viscosity, which diverges at a lower particle volume fraction as ionic strength increases, corresponding to a decrease of the effective particle volume fraction [23].

However, the novelty here, is to investigate the impact of ionic strength, not in pure electrosterically stabilized dispersions but in the presence of weak attractive depleting forces inferred by the addition of a non-absorbent polymer, namely polyethyleneoxide (PEO). Understanding how the strength and range of the repulsive interactions changes the effect of weak attractive interactions on phase behavior and flow in various particle concentration regimes will be discussed here for the first time. It is also worth mentioning, that all transition phenomena described in this study are different from the so-called re-entry glass transition phenomena reported earlier [24,25], since we focus on the transition from the fluid to fluid/crystalline co-existence and finally to the gel state. They are also different from the re-entry phenomenon described by Kumar et al. [26] for charge-stabilized silica nanoparticles. They observed aggregation of primary particles into fractal structures upon addition of non-absorbing polymer due to attractive depletion interaction. At higher polymer concentration, they found a re-dispersion of particles resulting in a homogeneous fluid state and attributed this to the dominant effect of repulsion among polymer molecules. This re-entry behavior was found to strongly depend on the ionic strength of the dispersion with a broader polymer concentration range of aggregation observed at higher ionic strength. The intricating effects of temperature on the complex phase behavior of colloidal dispersions with depletion attraction have been discussed by Feng et al. [27]. They have used ultra-high molecular weight PEO as depletion agent and upon variation of temperature the PEO changes from non-adsorbing to bridging of the particles and this has dramatic consequences on the phase behavior. Such phenomena, however, can be excluded here, since our experiments were performed at room temperature as well as moderate ionic strength and such the solubility of the PEO is not altered.

The colloidal system investigated consists of neutralized aqueous dispersions of poly (styrene-butyl acrylate) P(S/BA) particles of radius 130 nm, supplied by BASF SE. The dispersions were made using classical emulsion polymerization and acrylic acid was used as a surface functional co-monomer. Weak attractive particle interactions were introduced by adding small amounts of polyethylene oxide (PEO) (0–25 g/l) of molecular weight M_w=20 kDa and the ionic strength was varied by

the addition of natrium chloride (NaCl) at concentrations of 10 and 100 mM.

In the first part of this study, we discuss the effect of ionic strength on flow properties of dispersions with only repulsive interactions, namely without addition of PEO, using classical rotational rheometry. In particular, we study the impact of salt on the dispersion's viscosity below and above the hard sphere freezing point ($\phi_c = 0.5$) and the corresponding change in effective particle volume fraction ϕ_{eff}. In the second part, we focus on the ionic strength effect on dispersions where attractive interactions are induced by the addition of non-adsorbing polymer PEO. We investigate two particle concentration regimes. First, at particle volume fractions below the hard sphere freezing point ($\phi_c < 0.5$), namely in the fluid sate and then at volume fractions ($0.5 < \phi_c < 0.55$) corresponding to the fluid / crystalline coexistence region.

In both regimes, we characterize the macroscopic flow behavior of the dispersions using classical shear rheometry, whereas the multiple particle tracking (MPT) technique is used to characterize microstructural and local mechanical properties of the dispersions. In particular, the viscosity of the fluid phase (η_{fluid}), the fraction and size of the crystalline regions as well as their shear modulus ($G_{0,MPT}$) are determined. Results will enable us to establish correlations between macroscopic flow behavior and microstructure of the dispersions depending on the strength and range of colloidal interactions under different ionic strength conditions.

2. Materials and methods

2.1. Sample preparation

The system investigated is an aqueous colloidal dispersion of poly (styrene-butyl acrylate) P(S/BA) particles of radius 130 nm and polydispersity below 3 % provided by BASF SE. The sample was made using classical emulsion polymerization and acrylic acid was used as a functional co-monomer at a concentration of 2 %wt relative to the total monomer concentration resulting in a thin "hairy" surface layer (5 nm) providing electrosteric repulsion among particles. More details on the system are found in [1,14,28].

The particle volume fraction ϕ was calculated from the solids content $x_{particle}$ and the measured density of the dispersion $\rho_{dispersion}$ as $\phi = \frac{(x_{particle} * \rho_{dispersion})}{\rho_{particle}}$. Since the true surface charge in these dense colloidal dispersions and the thickness of the "hairy" surface layer is hard to access, the range of repulsive interaction was characterized through the effective volume fraction ϕ_{eff} which was determined from the divergence of the relative zero-shear viscosity $\eta_{rel} = \frac{\eta_0}{\eta_s}$ as a function of particle volume fraction ϕ. Here η_0 and η_s are the zero-shear viscosity and solvent viscosity, respectively. Fitting the empirical Maron & Pierce model [29]:

$$\eta_{rel} = \frac{\eta_0}{\eta_s} = \left(1 - \frac{\phi}{\phi_g}\right)^{-2} \quad (1)$$

to a set of $\eta_{rel}(\phi)$ data obtained at $\phi < 0.5$ yields an experimental value for the colloidal glass transition volume fraction $\phi_{g,\exp}$ and relating this parameter to the hard sphere colloidal glass transition $\phi_{g,HS} = 0.58$ provides the effective volume fraction:

$$\phi_{eff} = \phi\left(\frac{\phi_{g,HS}}{\phi_{g,\exp}}\right) \quad (2)$$

The system without added salt was investigated earlier [1], but was reproduced for comparison. The focus of our study is on the effect of varying ionic strength and the corresponding change in the range of electrosteric repulsion on structure and flow behavior of the dispersions when additional weak depletion attraction among the particles is present. For that, after an initial dialysis of the raw dispersion against a 10 mM NaCl solution for purification, the ionic strength was adjusted by adding to this solution, 10 mM and 100 mM NaCl, respectively. The range of the repulsive interaction, characterized by the Debye length was estimated from the measured conductivity of the dispersions and the known concentration dependence of the conductivity for NaCl solutions. Results obtained for the dispersions before and after dialysis as well as according to the NaCl content are shown in Table 1.

Table 1
Effect of the addition of salt (NaCl) on the dispersion's specifications at a constant volume fraction ϕ=0.45. I (M)= (σ(μS/cm)-119) / 82111 (calibration equation for NaCl) and κ^{-1}(nm)=0.304/$\sqrt{I(M)}$.

Sample	ϕ vol. fract.	Dialysis against NaCl	NaCl added mM	Conductivity σ / μS/cm	Ionic strength I / M	Debye-length κ^{-1} / nm
D_{raw}	0.45	No	-	2170	0.025	1.92
D_0	0.45	10 mM	0	2820	0.033	1.68
D_{10}	0.45	10 mM	10	4900	0.058	1.26
D_{100}	0.45	10 mM	100	9500	0.110	0.90

Table 2
Investigated PEO concentrations and resulting depletion interaction energy Ψ_{dep} / k_BT for the dispersion with a polymer-to-particle size ratio $\xi = R_g/a$=0.0485. R_g being the radius of gyration estimated at 6.3 nm according to Kawaguchi et al. [31].

ϕ_{PEO} in g/l	3	5	10	12	13	15	17	20	25
Ψ_{dep} / k_BT	2.9	4.9	9.8	11.7	12.7	14.6	16.6	19.5	24.4

The particle volume fraction of the raw dispersion provided by BASF SE was 0.48±0.01, therefore dispersions with $\phi < 0.5$ have simply been prepared by dilution of this stock dispersion and purification via dialysis. For that, a Spectral/Por® 4 dialysis membrane with a molecular weight cut-off (MWCO) of 12–14 kg/mol was used.

For dispersions with $\phi > 0.5$, a dialysis membrane with a molecular weight cut-off of 3.5 kDa was filled with the dispersion and immersed in a dialysis bath filled with an aqueous solution of PEO, $M_w = 35$ kDa, at a concentration of 15 %wt. The high osmotic pressure of the PEO solution concentrates the dispersion to the desired ϕ. Then for all dispersions, the pH was adjusted to 7 by adding 1 M NaOH.

Finally, non-adsorbing PEO (Merck, Germany) with a molecular weight of 20 kDa was added to the samples in different concentrations to introduce weak attractive depletion interactions. PEO was varied between 3 and 25 g/l, according to Asakura and Oosawa [30], this corresponds to a range of depletion attraction strength between 3 and 25 k_BT. Table 2 shows all of the data. It has to be mentioned here that for the calculation of the depletion interaction energy, we assumed a constant radius of gyration as a function of polymer concentration. However, the study of Zhou et al. [8] showed a reduction of this parameter with polymer concentration under good solvent conditions. Calculating the depletion energy based on this result would lead to a weaker increase in energy with polymer concentration than that obtained in our study by assuming a constant radius of gyration. Since this aspect does not affect the qualitative interpretation of our experimental findings, we do not address this aspect in further detail.

2.2. Macrorheology: rotational rheometry

A rotational rheometer (Physica MCR 501 from Anton Paar) equipped with concentric cylinders (CC10) or (CC27) measuring cells was used to perform steady shear measurements. The viscosity was obtained as a function of shear rate in a range from 0.1 to 1000 s^{-1}. All measurements were accomplished at a temperature of 20 °C and every measurement was preceded by a waiting time of 5 minutes to relax the

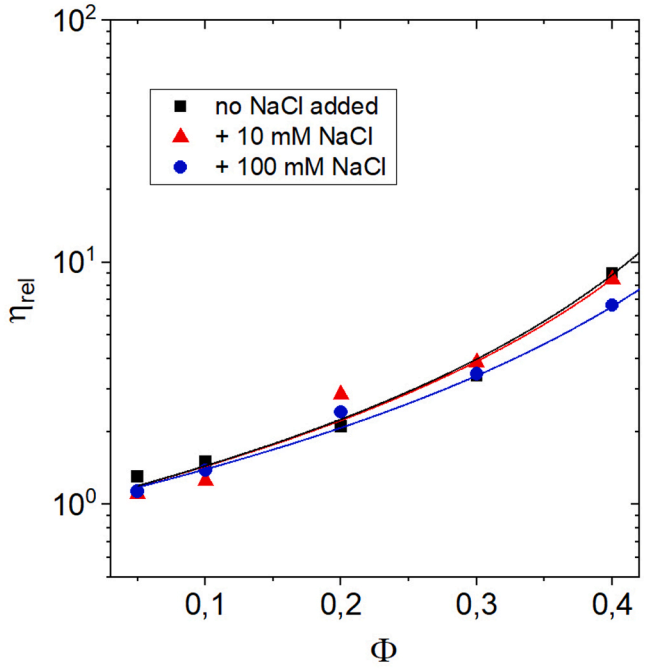

Fig. 1. variation of the relative viscosity as a function of particle volume fraction for dispersions without added NaCl (black square), with the addition of 10 mM (red triangle) and 100 mM (blue circle) NaCl, without added PEO. The solid line represents the empirical Maron&Pierce model.

residual stress produced by the filling process.

2.3. Microrheology: Multiple-particle tracking (MPT)

A detailed scheme of the MPT setup used in this study is described in Kowalczyk et al. [32]. It is based on an inverted fluorescence widefield microscope (Axio Observer D1, Carl Zeiss) equipped with a Fluar 100x objective (numerical aperture 1.3, 100x magnification, oil immersion lens, Carl Zeiss). Green fluorescent non-functionalized polystyrene microspheres of 0.2 μm diameter with density 1.06 g/cm^3 were used as tracer particles (Bangs Laboratories, USA). 2D images (field of view 127 ×127 μm, frame rate 50 frames/sec) of the fluorescent particles were recorded using a sCMOS camera Zyla X (Andor Technology). Movies of the fluctuating microspheres were analyzed using a custom MPT routine incorporated into the software Image Processing System (Visiometrics iPS) [33,34] which locates the center of mass $[x(t), \ y(t)]$ of each particle in every picture and allows the construction of particle trajectories. Individual time-averaged mean square displacements (MSD) were calculated according to a conventional MPT analysis, i.e. discarding all short particle trajectories composed of less than 50 frames, using a self-written Matlab® program based on the widely used Crocker and Grier tracking algorithm [32,35] with $\langle \Delta r^2(\tau) \rangle = \left\langle [x(t+\tau) - x(t)]^2 \right\rangle + \left\langle [y(t+\tau) - y(t)]^2 \right\rangle$ where τ is the time lag and t the elapsed time. Tracer particles incorporated into colloidal crystals exhibit a time-independent MSD directly related to the apparent local shear modulus of individual micron-sized crystals via the relationship [36]:

$$G_{0,MPT} = \frac{2k_B T}{3\pi a \langle \Delta r^2(\tau) \rangle} \quad (3)$$

with a being the tracer particle radius, k_B the Boltzmann constant, T the temperature and $\langle \Delta r^2(\tau) \rangle$ the constant MSD value. Tracers freely diffusing in a viscous environment exhibit a linearly increasing MSD and the apparent viscosity η_{MPT} of the surrounding fluid is determined using Eq. 4 obtained from the Stokes-Einstein relation [36] and the relation $\langle \Delta r^2(\tau) \rangle = 4D\tau$, where D is the diffusion coefficient related to the MSD $\langle \Delta r^2(\tau) \rangle$ as a function of the lag time τ [37]:

$$\eta_{MPT} = \frac{k_B T}{6\pi a D} \quad (4)$$

To characterize the heterogeneity of the dispersion microstructure, a statistical analysis of the MSD distribution was performed by extracting the non-Gaussian parameter $\alpha = \frac{\langle x^4(\tau) \rangle}{3\langle x^2(\tau) \rangle^2} - 1$, in which x^4 and x^2 are the fourth and second moments of the probability distribution of particle displacement [38]. For a Gaussian distribution $\alpha = 0$, as expected for an ergodic homogeneous, uniform sample, while deviations from this behavior like in heterogeneous samples result in large α values.

Beside this classical MPT analysis, we also produced the so-called image overlay which include all trajectories generated during a tracking experiment [1,39]. The result is simply the superposition of all particle trajectories across all images of the video sequence, here providing an accurate and direct visualization of the dispersion microstructure in terms of fluid, crystalline or gel-like regions.

3. Results and discussion

3.1. Ionic strength effect on flow properties of dispersions with only repulsive interactions

It is worth mentioning that in this study, the particle volume fraction ϕ considered, corresponds to the nominal volume fraction calculated from the weight and density of the suspended particles. Fig. 1 shows the variation of the relative viscosity $\eta_{rel} = \frac{\eta_0}{\eta_s}$ as a function of particle volume fraction $\phi < 0.5$ for PEO-free dispersions without addition of NaCl and with 10 mM and 100 NaCl added. The zero-shear viscosity η_0 was obtained in the shear rate regime at $\dot{\gamma} < 1s^{-1}$.

We observe, at low particle volume fractions (ϕ<0.4), that increasing ionic strength hardly affects the relative viscosity within experimental error. In this low volume fraction regime, the impact of the ionic strength on η_{rel} is almost insignificant. This is expected since in this case the average particle separation is larger than the range of colloidal interactions.

At higher particle volume fractions (ϕ>0.4), however, we see a weak but systematic decrease of the relative shear viscosity with increasing salt content. This effect is well known and is due to a reduced range of electrosteric repulsion between particles, corresponding to a reduction of the effective particle volume fraction ϕ_{eff}. Accordingly, for the dispersion with 100 mM NaCl added (blue symbols), η_{rel} diverges at a slightly higher ϕ value, indicating that its effective volume fraction is lower than for the other samples. Using Eq.1 and considering the experimental incertitude, we find $\phi_{g,\exp}$ =0.57±0.02, 0.58±0.02 and 0.61±0.03 for dispersions without added salt, with 10 mM and 100 mM added salt, respectively. Using these values and Eq. 2, we obtain, as an example for the raw dispersion with ϕ=0.48±0.01, ϕ_{eff} values of 0.49 ±0.02, 0.48±0.02 and 0.46±0.02, respectively. Although all these values appear similar within experimental error, we can still notice a slight systematic decrease of ϕ_{eff} with increasing ionic strength, as expected [40].

In summary, we have shown that for dispersions with only repulsive interactions, i.e without addition of PEO, at low particle volume fractions, the ionic strength has no impact on dispersions flow properties while at higher volume fractions, a slight decrease in viscosity with increasing ionic strength is observed due to a slight reduction of the effective volume fraction ϕ_{eff}, as expected.

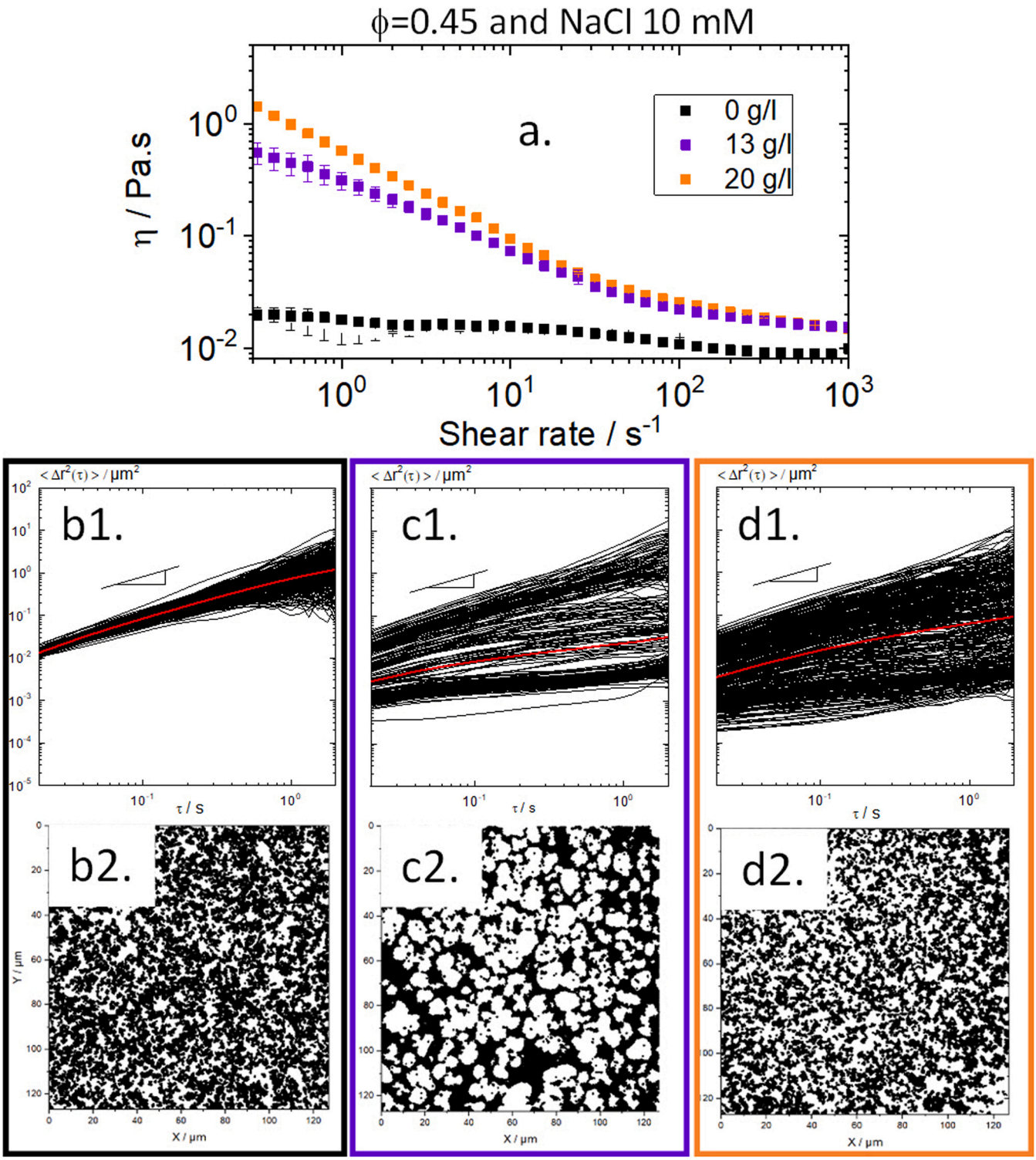

Fig. 2. 10 mM NaCl added. (a) Viscosity of the dispersion (ϕ= 0.45) as a function of shear rate without added polymer (black squares), and with 13 g/l (purple squares) and 20 g/l (orange squares) non-adsorbing polymer PEO, respectively. MPT microrheology results obtained for the dispersion without added polymer, and with 13 g/l and 20 g/l PEO with tracer particles of radius 105 nm. Frames are color coded according to the colors in (a). Upper row: mean square displacements (MSDs) of individual polystyrene microspheres as a function of lag time. Lower row: Overlay of 500 subsequent 127 × 127 μm images.

3.2. Ionic strength effect on dispersions including attractive interactions

3.2.1. Fluid state at $\phi < 0.5$

Here, we focused on the effect of ionic strength on dispersions with weak attractive attractions in the fluid state. It is worth mentioning here that whatever the salt content, for all dispersions, the effective volume fraction ϕ_{eff} is below the hard-sphere freezing point. Figs. 2 and 3 show the steady shear viscosity as a function of shear rate, the time-dependence of the MSDs, and an overlay of 500 subsequent images covering a time period $\Delta\tau$=10 s for dispersions with different concentrations of non-adsorbing polymer (PEO) in presence of 10 mM and 100 mM NaCl, respectively. Results obtained for dispersions without

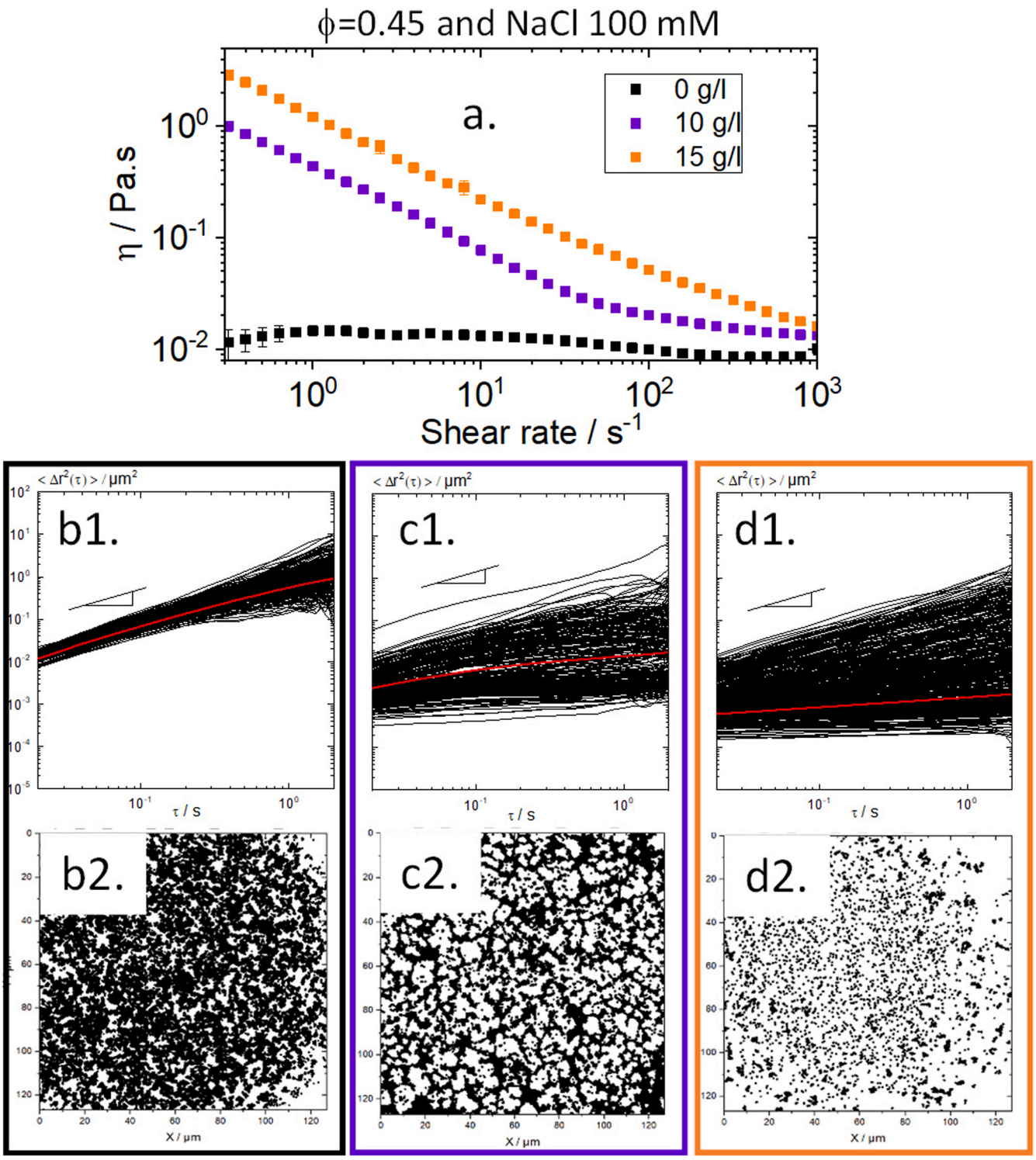

Fig. 3. 100 mM NaCl added. (a) Viscosity of the dispersion (ϕ= 0.45) as a function of shear rate without added polymer (black squares), and with 10 g/l (purple squares) and 15 g/l (orange squares) non-adsorbing polymer PEO, respectively. MPT microrheology results obtained for the dispersion without added polymer, and with 10 g/l and 15 g/l PEO with tracer particles of radius 105 nm. Frames are color coded according to the colors in (a). Upper row: mean square displacements (MSDs) of individual polystyrene microspheres as a function of lag time. Lower row: Overlay of 500 subsequent 127 × 127 μm images.

added salt have already been published in Weis et al. [1] and the characteristic features of these systems that we also measured are shown for comparison in Table 1 and in the supplementary (S1). Independent of salt concentration, when no polymer is added, both dispersions are in the fluid state with an almost similar low zero-shear viscosity of around 16.0±2.0 mPa.s and a weak shear-thinning behavior (black symbols in Figs. 2a and 3a, respectively). The variation of individual MSDs for both samples are shown in figures 2b1 and 3b1, respectively. A similar behavior is observed, namely that all MSDs lie in a narrow range and vary almost linearly with time indicating that the motion of the tracer particles is purely diffusive and that the microenvironment surrounding the particles responds like a viscous liquid. From the average MSD of all linear MSDs and using Eq. 4, the local viscosity within the fluid $\eta_{MPT} = \eta_{fluid}$ was determined to be 12.0±3.0 mPa.s which is in fair agreement

Table 3
Characteristic data for dispersions with particle volume fractions ϕ=0.45 and different polymer concentrations and ionic strength conditions. Shear viscosity η is determined at $\dot{\gamma}$=1 s^{-1} from bulk rheometry, η_{fluid}, $G_{0,MPT}$, ϕ_{fluid} and $\phi_{crystal}$ are deduced from MPT.

NaCl	ϕ_{PEO}	Phase	η ($\dot{\gamma}$=1 s^{-1})	η_{fluid} (slope 0.9–1)	Crystal size	$\phi_{crystal}$	ϕ_{fluid}	$G_{0,MPT}$
mM	g/l	state	mPa.s	mPa.s	μm			Pa
0	0–17	fluid	17±2	12.0±3	-	-	-	-
	20							
	25							
	20	fluid/crystal	300±30	10.7±6.7	17.7±5.5	0.60±0.06	0.36±0.05	6.1±3.0
	25	gel	3000±300	13.5±5	-	-	-	-
10	0–12	fluid	16±2	10±2	-	-	-	-
	13	fluid/crystal	310±30	13.4±10	11.7±2.7	0.51±0.04	0.39±0.05	5.8±3.3
	20	gel	600±60	13.2±11	-	-	-	-
100	0–5	fluid	14±1	9±2	-	-	-	-
	10	fluid/crystal	450±45	36.6±25.7	7.7±2.3	0.44±0.03	0.46±0.03	6.5±3.6
	15	gel	1260±65	157±85	-	-	-	-

with the 16.0±2.0 mPa.s determined macroscopically.

The statistical analysis of the MSD distribution clearly reveals a homogeneous structure in both cases with a non-Gaussian parameter α close to zero. In both cases, overlay images also are almost uniformly black, as shown in Figures 2b2 and 3b2, respectively, indicating that the tracers are freely diffusing, exploring the whole sample.

Introducing weak attraction by adding non-adsorbing polymer PEO in both cases leads to an increase in the zero-shear viscosity and more pronounced shear thinning. For samples with 10 mM NaCl (Fig. 2a), the viscosity remains low, around 16.0±2.0 mPa.s and almost constant with shear rate (data not shown) until 13 g/l PEO is added. At this polymer concentration the viscosity strongly increases, by a factor >10, and a strong shear thinning behavior is observed. A similar transition takes place for samples with 100 mM NaCl (Fig. 3a) but occurs at a lower PEO concentration, namely 10 g/l. For the system without added salt, the increase in viscosity was observed to occur at a PEO concentration of 20 g/l (Table 3 and S1). Thus, this first structural transition corresponding to a strong increase in viscosity, occurs at a lower PEO concentration, i.e. at a weaker depletion attraction, when salt is added to the dispersion, i.e. when the thickness of the hairy surface layer and hence the strength of electrosteric repulsion decreases.

As for systems without added salt [1], in presence of NaCl, this transition is due to the change from a homogeneous fluid to a fluid-crystalline regime. This assertion is confirmed by visual inspection of the samples which reveals the opalescent characteristic of the colloidal crystals. In addition, MPT reveals a broad variation in absolute values and time dependence of the individual MSDs. Time-independent MSDs corresponding to some tracers trapped in the crystalline regions whereas MSDs increasing linearly corresponds to tracers freely diffusing in the fluid regions. See Figures 2c1 and 3c1 for solutions with 10 mM and 100 mM NaCl, respectively. The modulus of the colloidal crystals $G_{0,MPT}$ determined using Eq. 3 is found to be 6.1±3.0 Pa, 5.8±3.3 Pa and 6.6±3.6 Pa in solutions without added salt (S1c1), with 10 mM and 100 mM NaCl added, respectively. This result seems to indicate that within experimental error the modulus of the individual crystals does not depend on ionic strength. The overlay images show the size and shape of the crystalline regions represented by the white areas, whereas black areas represent the fluid regions. A decrease of the characteristic length scale of the crystalline structure is observed from 17.7± 5.5 μm for dispersions without NaCl added (Table 3 and S1c2) to 11.7± 2.7 μm in presence of 10 mM NaCl (Fig. 2c2), reaching 7.7± 2.3 μm for solutions with 100 mM NaCl added (Fig. 3c2). This reduction in crystal size with increasing ionic strength is accompanied by a reduction of the particle density in the crystal domains $\phi_{crystal}$ and at the same time an increase in viscosity within the fluid phase η_{fluid}. We obtain η_{fluid}=10.7 ±6.7 mPa.s and $\phi_{crystal}$=0.60±0.06 in dispersions without added salt, 13.4±10 mPa.s and 0.51±0.04 with 10 mM NaCl and 36.6±25.7 mPa.s and 0.44±0.03 with 100 mM NaCl added, respectively. The relatively large error bars obtained for viscosity values are due to the broad distribution of MSD slopes as well as absolute values as shown in Figures S1c1, 2c1 and 3c1. The determination of $\phi_{crystal}$ has been obtained from MPT data using the area fraction A_{fluid} pervaded by the tracer particles (black areas in the overlay image) and, assuming that this quantity represents the fraction of the dispersion that is in the fluid state, we can set:

$$\phi = A_{fluid}.\phi_{fluid} + (1 - A_{fluid})\phi_{crystal} \quad (5)$$

with ϕ_{fluid} being the particle volume fraction of the fluid phase calculated using Eq. 1 by replacing η_0 by η_{fluid} and where η_{fluid} is determined from the MSDs of the freely-diffusing tracers, having a slope between 0.9 and 1, using Eq. 4. Characteristic data extracted from all these experiments performed on dispersions without added salt, with 10 mM and 100 mM salt (NaCl) added, are summarized in Table 3.

In summary, we find that the transition from a homogeneous fluid to a fluid-crystalline regime is more difficult to initiate in the case of dispersions without added salt, it requires a significantly higher amount of PEO corresponding to stronger attraction forces and leads to the formation of large dense crystals with a relatively low viscosity of the fluid phase. In presence of NaCl, less polymer is needed for the transition which means that attraction forces necessary to induce crystallization are weaker, leading to a reduction in the size and density of the crystals and an increase in the fluid viscosity. We can suppose that this behavior can be attributed to a combined effect between the addition of non-adsorbent polymer inducing depleting attractive forces with at the same time a decrease of the repulsive interactions among particles with increasing ionic strength as was demonstrated by the reduction of ϕ_{eff}. In presence of salt, less polymer is therefore needed to induce the phase transition.

When the polymer concentration is further increased, a second transition occurs. The opalescence disappears and the steady-shear viscosity further increases with a shear thinning behaviour slightly more pronounced. This is characteristic of an attractive gel. This transition occurs at PEO concentrations of 20 g/l and around 15 g/l for solutions with 10 mM and 100 mM NaCl, respectively (see Figs. 2a and 3a). For systems without added salt, this second transition occurs at a PEO concentration of 25 g/l (Table 3 and S1a). Again here, as for the first transition, increasing ionic strength makes this second transition occurring at lower PEO concentration due to a reduction of the repulsive interactions. MPT experiments again show a broad variety of MSDs with

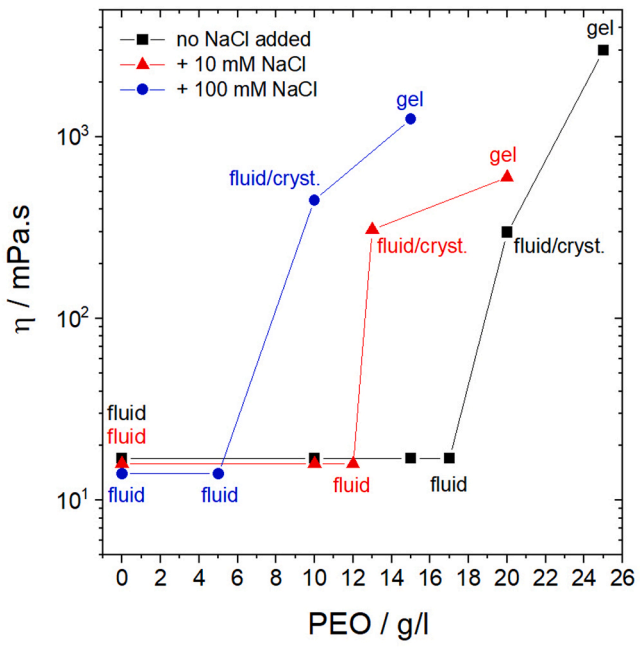

Fig. 4. Phase diagram for dispersions at Φ=0.45 upon adding non-adsorbing polymer PEO for different amounts of added NaCl. The horizontal axis represents the concentration of added PEO polymer and the vertical axis the bulk shear viscosity determined at a shear rate of 1 s^{-1}. Fluid, fluid/crystalline coexistence and gel states were identified as described in Section 3.2.

different absolute values and slopes. The heterogeneous microstructure of this gel state with its dense (white) and less dense (black) regions is seen in the overlay images, which indicates a much finer microstructure than for the fluid/crystalline state observed at a lower PEO concentration. This fine gel structure appears more pronounced and uniform in the presence of 100 mM NaCl (Fig. 3d2) than with 10 mM NaCl (Fig. 2d2). In the latter case, the heterogeneous structure more closely resembles a percolated network of dense, small regions with a size of 6.7±2.7 μm, and a low viscosity η_{fluid} =13.2±11 mPa.s, i.e. low particle density in the fluid regions of the heterogeneous gel. The viscosity determined from freely diffusing tracer particles for the gel formed from the dispersion with 100 mM added NaCl is η_{fluid} = 157±85 mPa.s. Despite its large uncertainty this indicates, that the particle density is more uniform in this case.

In conclusion, we have shown that, below the hard sphere freezing point (ϕ_c < 0.5), starting from the fluid state, the evolution of the dispersion when adding PEO remains the same in both the absence and presence of salt. The dispersion successively goes through two transitions, namely fluid to fluid/crystal coexistence and fluid/crystal coexistence to gel. However, increasing the ionic strength shifts concentrations of both phase transitions, which occur at lower polymer concentrations when ionic strength is higher. Furthermore, the PEO concentration range of fluid/crystalline coexistence systematically decreases with increasing salt content. Fig. 4 illustrates these findings by representing the complete phase diagram of dispersions at ϕ = 0.45 upon adding non-adsorbing polymer PEO for different amount of added NaCl salt. Furthermore, the size and the particle density of the crystals decreases with increasing salt concentration. The gel structure occurring at higher attractive strength is distinctly heterogeneous at low concentration of added salt, whereas overlay images reveal a more uniform gel state at high salt content.

3.2.2. *Fluid-crystalline coexistence regime*

In this section, we investigate the impact of ionic strength on dispersions with weak attractive attractions in the fluid/crystalline coexistence regime. For the dispersion without added salt, ϕ = 0.52 corresponds to a value of ϕ_{eff}= 0.53±0.02 which means that the initial state of this sample is well in the fluid/crystalline coexistence regime when no PEO is added. This is directly evident from the opalescent appearance of the sample, but it is also visible from the MPT overlay image (S2b2). As expected [41], the addition of PEO leads to a broadening of the coexistence range. The particle concentration in the fluid phase decreases and crystal density increases monotonically with increasing PEO content, i.e. increasing attraction strength (Table 4). MPT experiments also show, that the size of the crystals changes with PEO concentration: at a PEO concentration of 3 g/l the crystals are larger (14.5±3.8 μm) than those obtained in both dispersions without added PEO (7±1.5 μm) and with 10 g/l (9.4±2 μm) PEO content. These microstructural features result in a pronounced shear thinning behavior and a minimum low shear viscosity is observed at 3 g/l PEO concentration (Fig. S2a). MPT data allow for a determination of the fluid phase viscosity and the volume fraction of suspended crystals. Based on these data, the observed viscosity minimum can be rationalized simply treating the systems as hard sphere dispersions of crystals in a Newtonian dispersion of primary colloidal particles with particle concentration and hence solvent viscosity varying with added PEO. In this study, these findings are less pronounced but consistent with the previously published data [1] and are shown here as Supplementary Information (Fig. S2).

Here, we focus on the effect of added salt on these microstructural variations and their consequences for bulk viscosity. In presence of 10 mM NaCl, ϕ = 0.52 corresponds to a ϕ_{eff}= 0. 52±0.02 which is just above the hard sphere freezing point. The shrinkage of the hairy surface layer has a significant effect on microstructure and bulk viscosity when

Table 4
Characteristic data for dispersions with particle volume fractions ϕ=0.52 and different polymer concentrations and ionic strength conditions. Shear viscosity η is determined at $\dot{\gamma}$=1 s^{-1} from bulk rheometry, η_{fluid}, $G_{0,MPT}$, ϕ_{fluid} and $\phi_{crystal}$ are deduced from MPT.

NaCl	ϕ_{PEO}	Phase	η ($\dot{\gamma}$=1 s^{-1})	$\eta_{fluid\ (slope\ 0.9–1)}$	Crystal size	$\phi_{crystal}$	ϕ_{fluid}	$G_{0,MPT}$
mM	g/l	state	mPa.s	mPa.s	μm			Pa
0	0	fluid/crystal	98±11	54±24	7±1.5	0.53±0.01	0.48±0.02	9.7±5.0
	3	fluid/crystal	53±5	34±17	14.5±3.8	0.54±0.01	0.46±0.02	9.0±5.0
	10	fluid/crystal	106±4	31±13	9.4±2	0.55±0.01	0.45±0.02	9.8±5.4
10	0	≤fluid/cryst.	60±5	21±7	-	-	-	-
	3	fluid/crystal	95±6	21±14	34±5	0.56±0.04	0.43±0.04	9.9±2.1
	10	fluid/crystal	180±3	17±7	38±5	0.61±0.04	0.41±0.04	9.4±4.7
100	0	fluid	47±6	14±4	-	-	-	-
	3	fluid/crystal	1065±151	19±11	9.5±3	0.60±0.04	0.42±0.03	4.4±2.7
	10	gel	995±445	334±260	-	-	-	-

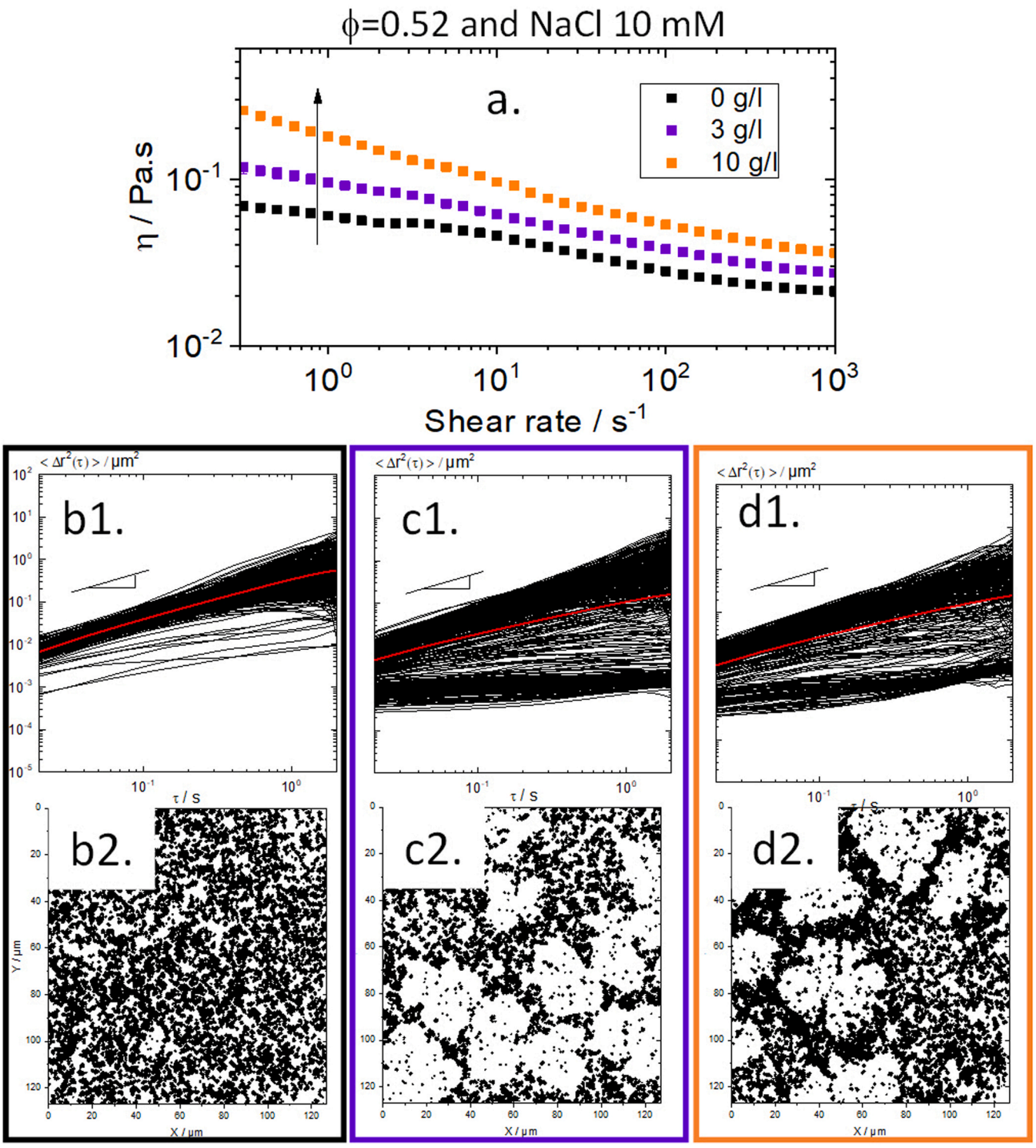

Fig. 5. 10 mM NaCl added. (a) Viscosity of the dispersion (ϕ= 0.52) as a function of shear rate without added polymer (black squares), and with 3 g/l (purple squares) and 10 g/l (orange squares) non-adsorbing polymer PEO, respectively. MPT microrheology results obtained for the dispersion without added polymer, and with 3 g/l and 10 g/l PEO with tracer particles of radius 105 nm. Frames are color coded according to the colors in (a). Upper row: mean square displacements (MSDs) of individual polystyrene microspheres as a function of lag time. Lower row: Overlay of 500 subsequent 127 × 127 µm images.

PEO is added. Results obtained for samples with 10 mM added NaCl are shown in Fig. 5. All samples exhibit shear thinning behaviour and no decrease or minimum in viscosity is observed with addition of PEO. Instead, we observe a continuous increase of the low shear viscosity with increasing PEO concentration (Fig. 5a). The viscosity measured at $\dot{\gamma} = 1s^{-1}$ increases from 60±5 mPa.s without PEO to 100±10 mPa.s to reach 180±20 mPa.s with the addition of 3 and 10 g/l of PEO, respectively.

The MPT data show that the dispersion without PEO and with 10 mM NaCl added (Fig. 5b1), in contrast to the system without addition of NaCl, (Fig. S2b1) essentially is in a fluid state. Most MSDs exhibit a linear variation as a function of lag time at least up to $\tau = 1$ s, i.e. the tracer particles freely diffuse, and the overlay image (Fig. 5b2) is almost uniformly black, indicating that the tracer particles are free to explore

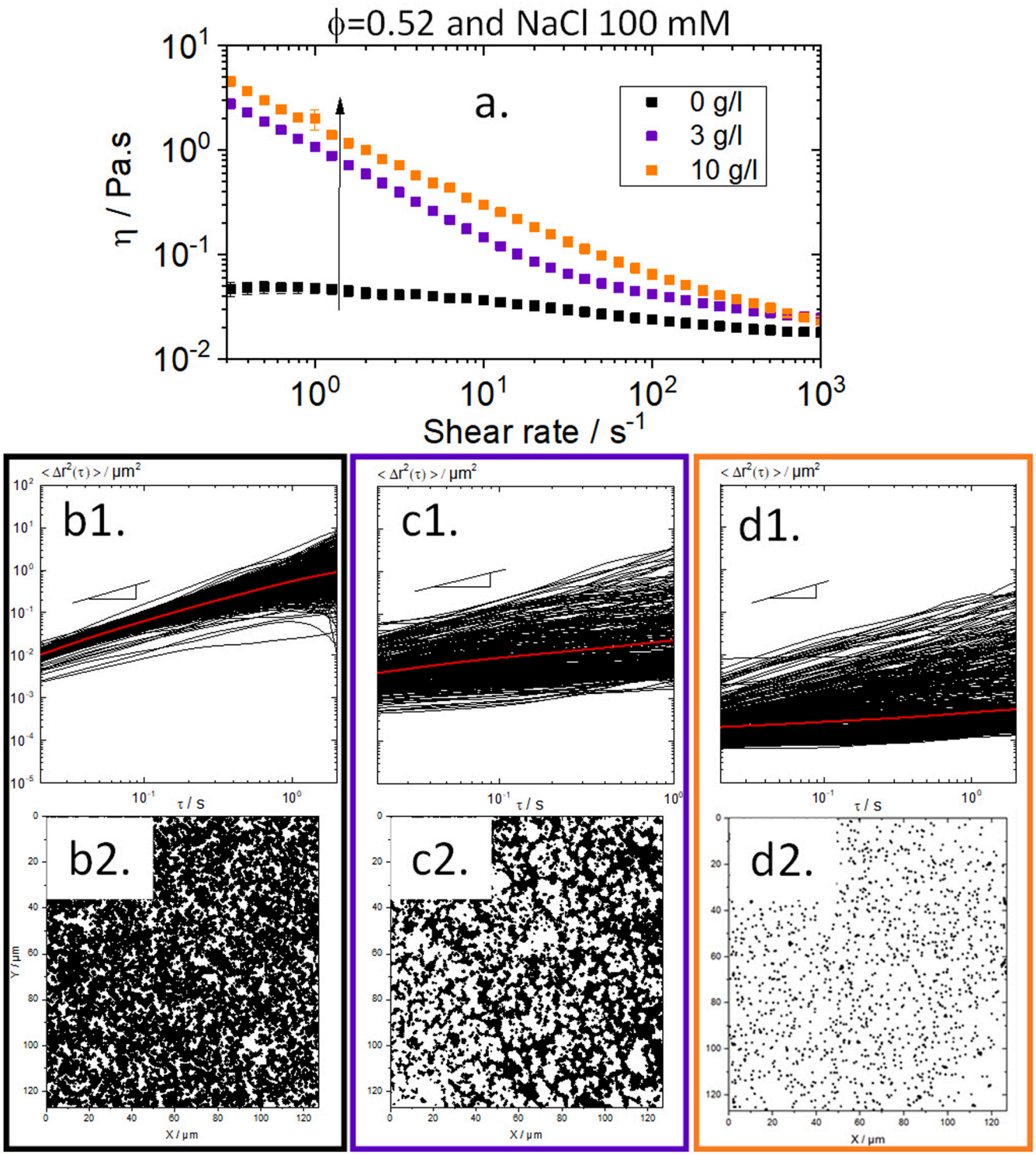

Fig. 6. 100 mM NaCl added. (a) Viscosity of the dispersion (ϕ= 0.52) as a function of shear rate without added polymer (black squares), and with 3 g/l (purple squares) and 10 g/l (orange squares) non-adsorbing polymer PEO, respectively. MPT microrheology results obtained for the dispersion without added polymer, and with 3 g/l and 10 g/l PEO with tracer particles of radius 105 nm. Frames are color coded according to the colors in (a). Upper row: mean square displacements (MSDs) of individual polystyrene microspheres as a function of lag time. Lower row: Overlay of 500 subsequent 127 × 127 μm images.

all regions of the sample. The value of the non-Gaussian parameter α is less than 1, indicating that the tracer particles explore a uniform environment. However, the local viscosity of the fluid η_{fluid} = 21±7 mPa.s determined based on Eq. (4) is three times less than the 60±5 mPa.s measured macroscopically. A closer look at the overlay image suggests the presence of few small individual white areas that could correspond to very small crystals and the particles trapped in these crystals do not contribute to η_{fluid}, but of course to the bulk viscosity.

The addition of only 3 g/l PEO to this dispersion leads to the formation of very large crystals of around 34±5 μm in size as shown in the figure 5c2, which corresponds to the viscosity increase shown in Fig. 5a. The formation of crystals with the addition of such a small amount of

Table 5
Characteristic data for dispersions with particle volume fractions ϕ=0.54 and different polymer concentrations without added salt (NaCl). Shear viscosity η is determined at $\dot{\gamma}$=1 s^{-1} from bulk rheometry, η_{fluid}, $G_{0,MPT}$, ϕ_{fluid} and $\phi_{crystal}$ are deduced from MPT.

NaCl	ϕ_{PEO}	Phase	η ($\dot{\gamma}$=1 s^{-1})	$\eta_{fluid\ (sl.0.9\text{-}1)}$	Crystal size	$\phi_{crystal}$	ϕ_{fluid}	$G_{0,\ MPT}$
mM	g/l	state	mPa.s	mPa.s	μm			Pa
0	0	fluid/crystal	1130±110	22±12	8.5±2	0.58±0.02	0.43±0.03	12±7
	3							
	10							
	15							
	3	fluid/crystal	985±98	27±15	12.5±3	0.57±0.01	0.44±0.03	12±8
	10	fluid/crystal	432±40	26±13	15.6±3	0.56±0.01	0.44±0.03	11±8
	15	fluid/crystal	953±95	25±15	10.5±3	0.56±0.01	0.44±0.03	11±8

PEO is evidence for the broadening of the fluid/crystalline coexistence regime in the presence of attractive interaction strength [41]. Obviously, a nominal interaction strength of about 2.93 k_BT is enough to induce the transition from the fluid state to the fluid/crystalline regime here.

Adding more PEO at 10 g/l does not change the average crystal size (Fig. 5d2) as well as their local shear modulus $G_{0,MPT}$ and fluid viscosity η_{fluid} within experimental error (Table 4). $G_{0,MPT}$ and η_{fluid} remain constant around 10±5 Pa and 20±10 mPa.s, respectively, irrespective of the polymer concentration. However, we observe a slight increase of the crystal density $\phi_{crystal}$ from 0.56±0.04–0.61±0.04 for dispersions with 3 g/l and 10 g/l PEO, respectively, which is probably responsible for the corresponding increase in bulk viscosity.

Results obtained for the dispersion at ϕ=0.52, in presence of 100 mM NaCl, are shown in Fig. 6. In this case, ϕ=0.52 corresponds to ϕ_{eff} = 0.49±0.02, a value just below the hard sphere freezing point. Here, the initial state without PEO is clearly a fluid state as confirmed by both the variation of MSDs (Fig. 6b1) and the overlay image (Fig. 6b2). In addition, both parameters, η_{fluid} = 14±4 mPa.s and η_0 = 47±6 mPa.s become lower and get closer, also confirming this fluid state.

Without added PEO, the viscosity of the 100 mM NaCl sample at a given solids content is slightly lower than that of the 10 mM NaCl sample since ϕ_{eff}decreases with increasing ionic strength. However, the increase of viscosity when adding PEO is much more pronounced in presence of 100 mM salt. The low shear viscosity, measured at $\dot{\gamma} < 1s^{-1}$, increases from 47±6 mPa.s without PEO to 1065±15 mPa.s reaching 1995±445 mPa.s with 3 g/l and 10 g/l PEO added, respectively (Fig. 6a). At similar PEO concentration, absolute values of the viscosity are by more than a factor of 10 higher for dispersions containing 100 mM NaCl than those with 10 mM NaCl. Based on the MPT results shown in Figs. 5 and 6, these results can be rationalized as follows:

The most significant difference is that for the dispersion with 100 mM NaCl, the overlay image obtained at 3 g/l (Fig. 6c2) shows the formation of much smaller crystals of size 9.5±3 μm compared to the sample with 10 mM NaCl and a crystal size of 34±5 μm.

Additionally, for the 100 mM dispersion, the fraction of crystalline regions is slightly higher and crystals are also more evenly distributed throughout the sample and seem to form a sample spanning network. This percolating network of small crystal seems to be the major reason for the high low shear viscosity. It should be noted, that the high shear viscosity of all samples with 10 or 100 mM NaCl and different concentration of added PEO lies in a narrow range corresponding to the constant total particle loading.

At 10 g/l PEO and 100 mM NaCl, macroscopic opalescence disappears and also in MPT experiments crystals are no longer observed (Figure 6d2). The behavior is that of a strongly shear thinning gel with a low shear viscosity slightly higher than that of the dispersion with the lower PEO content, i.e. weaker attractive interaction with its fluid/crystalline coexistence microstructure. Similar as for the samples with ϕ =0.45, the system with a shorter range of electrosteric repulsion, exhibits a narrower range of fluid/crystalline coexistence.

3.2.3. Gel state

At a particle volume fraction ϕ =0.54, we find distinctly different behavior of the sample without added salt and those with 10 and 100 mM NaCl added. Consistent with the results published in Weis et al. [1], for the sample without added salt with a ϕ_{eff}=0.55±0.02, the addition of PEO leads to the expected broadening of the fluid/crystalline co-existence regime and the formation of a minimum in low shear viscosity occurring at a polymer concentration of 10 g/l (Fig. S3a). Overlay images confirm the fluid/crystalline initial state with the formation of crystals with a size of 8.5±2 μm (Fig. S3b2) and a slight increase in their size with addition of PEO to reach a maximum of 15.6±3 μm at 10 g/l of PEO, which corresponds to the lowest bulk viscosity observed.

Data extracted from these experiments performed on dispersions without added salt, are summarized in Table 5. For dispersions containing 10 and 100 mM NaCl, ϕ_{eff} values of 0.54±0.02 and 0.52 ±0.03, respectively, have been determined. Nevertheless, these samples are not in the fluid/crystalline coexistence regime. None of these samples either with or without added PEO showed opalescence, and also MPT overlay images do not show any indication of the existence of crystalline regions (Fig. 7 b2, c2, d2 and Fig. 8 b2, c2, d2). So, we have to conclude that all these samples are in the gel state. Keeping in mind that ϕ_{eff} decreases with increasing ionic strength, we find that the width of the fluid/crystalline coexistence regime narrows down as the range of electrosteric repulsions decreases and the addition of PEO seems not to broaden the coexistence regime. The MPT data show that the distribution of MSD values at a given lag time clearly narrows with increasing PEO concentration, i.e. the gel structure becomes more uniform, and this effect is more pronounced for the system with higher ionic strength. Indeed, for dispersions with 100 mM NaCl added, the α value determined at a lag time of 0.1 s, decreases from 8 to 1 for samples without added PEO and with 10 g/l PEO content, respectively. Without PEO (Fig. 8b2), trajectories of freely diffusing as well as elastically trapped tracer particles are observed within the field of view and the characteristic length scale of heterogeneity is ≈25 μm. In contrast, for the sample with 10 g/l PEO added (Fig. 8d2), all tracers are elastically trapped and hence we conclude that the length scale of heterogeneity exceeds 130 μm.

The increasing uniformity is also evident from the viscosity η_{fluid} determined from the freely diffusing tracer particles. This quantity strongly increases with increasing PEO content, for both sample series with 10 mM and 100 mM added NaCl.

Concerning the impact of the addition of PEO on the low shear viscosity for dispersions in presence of 10 mM (Fig. 7a) and 100 mM (Fig. 8a) NaCl, in both cases, increasing the attraction strength has no significant effect on the bulk viscosity function. No significant change in viscosity is observed with the addition of PEO. Flow curves are almost similar with viscosity absolute values and degree of shear thinning essentially the same, independent of PEO concentration and salt content.

As already mentioned in the introduction, please note that all phase transitions observed in this study, both in the fluid state, the fluid/

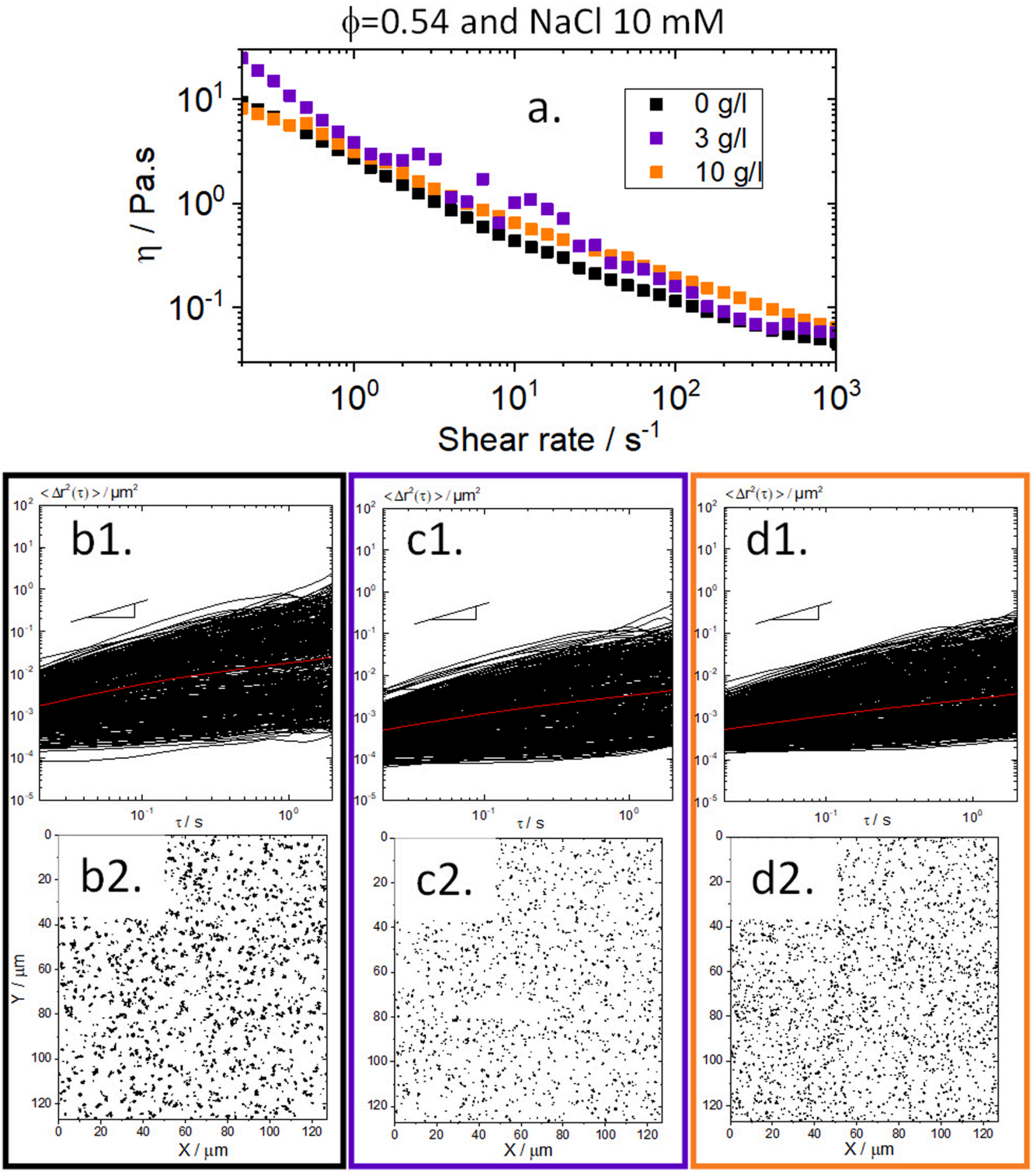

Fig. 7. 10 mM NaCl added. (a) Viscosity of the dispersion (ϕ= 0.54) as a function of shear rate without added polymer (black squares), with 3 g/l (purple squares) and 10 g/l (orange squares) non-adsorbing polymer PEO, respectively. MPT microrheology results obtained for the dispersion without added polymer, and with 3 g/l and 10 g/l PEO with tracer particles of radius 105 nm. Frames are color coded according to the colors in (a). Upper row: mean square displacements (MSDs) of individual polystyrene microspheres as a function of lag time. Lower row: Overlay of 500 subsequent 127 × 127 μm images.

crystalline coexistence regime as well as the gel state should not be confused with the so-called re-entrant phenomenon [26]. Indeed, in all cases here, after a first phase change, the system never returns back to its original phase.

4. Conclusion

In this study, we investigated the effect of ionic strength on the phase behavior, structure and flow properties of colloidal dispersions consisting of poly (styrene-butyl acrylate) P(S/BA) of radius 130 nm stabilized by short-range repulsive interactions. We investigated the impact

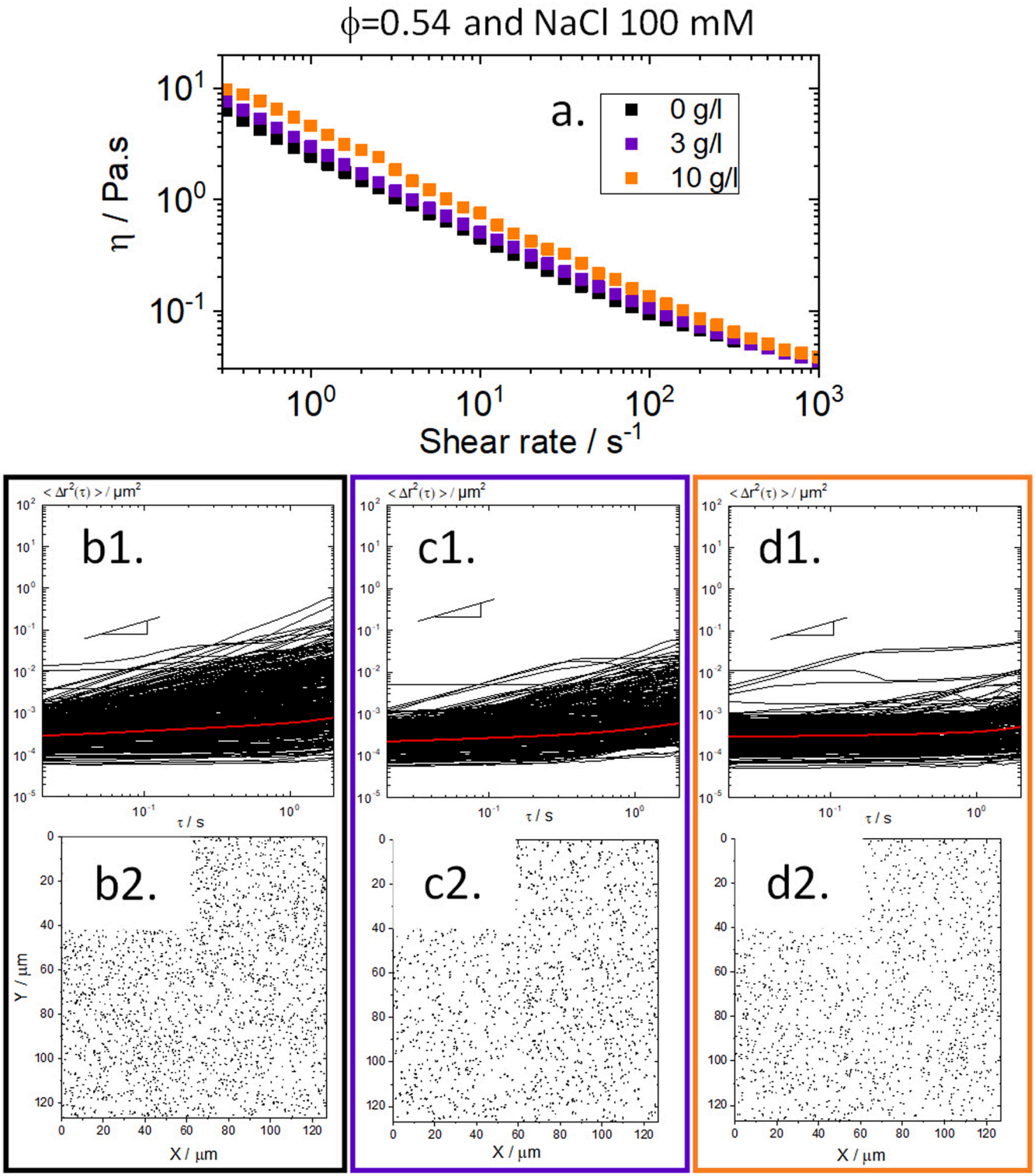

Fig. 8. 100 mM NaCl added. (a) Viscosity of the dispersion (ϕ= 0.54) as a function of shear rate without added polymer (black squares), with 3 g/l (purple squares) and 10 g/l (orange squares) non-adsorbing polymer PEO, respectively. MPT microrheology results obtained for the dispersion without added polymer, and with 3 g/l and 10 g/l PEO with tracer particles of radius 105 nm. Frames are color coded according to the colors in (a). Upper row: mean square displacements (MSDs) of individual polystyrene microspheres as a function of lag time. Lower row: Overlay of 500 subsequent 127 × 127 μm images.

of ionic strength, by varying the concentration of natrium chloride (NaCl), not only for dispersions with only repulsive interactions, but also when additional attractive depleting forces are present due to the addition of a non-absorbent polymer, namely polyethyleneoxide (PEO). These investigations provided new insight how superimposed short range electrosteric repulsion and weak depletion attraction affect microstructure and flow behavior of colloidal dispersions. For dispersions with only repulsive electrosteric interactions, at low particle volume fractions ($\phi < 0.4$), increasing ionic strength has almost no impact on the relative viscosity whereas at higher particle volume fractions, a

decrease in viscosity has been observed, as expected due to a reduced range of electrosteric repulsion between particles, corresponding to a reduction of the effective particle volume fraction ϕ_{eff}.

For dispersions including attractive interactions, at volume fractions ϕ=0.45 below the hard sphere freezing point (ϕ_c=0.5), irrespective of ionic strength, the bulk viscosity increases monotonically with increasing PEO concentration, i.e. attraction strength, due to the transition from a fluid to a fluid/crystalline and finally to a gel state. However, the increase in ionic strength shifts the concentrations of both phase transitions to lower polymer concentrations, indicating that in presence of salt a weaker attraction is required to induce these transitions. This phenomenon results in a decrease in size and packing density of the microcrystals formed in the fluid/crystalline coexistence regime as the ionic strength increases with at the same time a slight increase of the viscosity within the fluid phase η_{fluid} and a constant elastic modulus within the crystals $G_{0,MPT}$.

At ϕ=0.52, just above ϕ_c, for dispersions without added salt, broadening of the fluid-crystalline coexistence regime, due to added PEO, results in a viscosity minimum corresponding to different size and packing density of the crystalline regions as reported earlier [1]. In presence of salt, no viscosity minimum is observed when PEO is added. On the contrary, the addition of PEO leads to a continuous increase in bulk viscosity, similar to the case ϕ= 0.45. This result is explained by a shift of the initial phase without PEO from the fluid/crystalline regime to the fluid state due to the reduction of ϕ_{eff} as the ionic strength increases. From this initial state, only 3 g/l polymer is required to induce the formation of large crystals of size ≈35 μm for dispersions containing 10 mM NaCl and a network of small, dense crystals of size ≈10 μm with 100 mM NaCl. At ϕ=0.54, a result similar to ϕ=0.52 is obtained for dispersions without added salt, whereas in presence of salt, we find that the fluid/crystalline coexistence regime narrows down as the range of electrosteric repulsions decreases and the addition of PEO induces the formation of a gel state. This heterogeneity of the observed gels decreases with increasing PEO concentration, but absolute viscosity values and the degree of shear thinning remain unaffected.

CRediT authorship contribution statement

Marc Müller: Investigation. **Louise Ratel:** Investigation. **Norbert Willenbacher:** Writing – review & editing, Supervision. **Bruna Regina Maciel:** Supervision, Investigation. **Claude Oelschlaeger:** Writing – review & editing, Writing – original draft, Supervision, Investigation.

Declaration of Competing Interest

The authors declare that they have no known competing financial interests or personal relationships that could have appeared to influence the work reported in this paper.

Data availability

No data was used for the research described in the article.

Acknowledgements

The authors thank BASF SE for donating the styrene–butylacrylate model latex and the financial support by German Research Foundation DFG grant WI 3138/32–1.

Appendix A. Supporting information

Supplementary data associated with this article can be found in the online version at doi:10.1016/j.colsurfa.2024.134694.

References

[1] C. Weis, C. Oelschlaeger, D. Dijkstra, M. Ranft, N. Willenbacher, Microstructure, local dynamics, and flow behavior of colloidal suspensions with weak attractive interactions, Sci. Rep. 6 (2016) 33498.
[2] E. Zaccarelli, Colloidal gels: equilibrium and non-equilibrium routes, J. Phys.: Condens. Matter 19 (2007) 323101.
[3] K. Schätzel, B. Ackerson, Observation on density fluctuations, Phys. Rev. Lett. 68 (1992) 337–340.
[4] G. Hunter, E. Weeks, The physics of colloidal glass transition, Rep. Prog. Phys. 75 (2012) 066501.
[5] Z. Cai, Z. Li, S. Ravaine, M. He, Y. Song, Y. Yin, H. Zheng, J. Teng, A. Zhang, From colloidal particles to photonic crystals: advances in self-assembly and their emerging applications, Chem. Soc. Rev. 50 (2021) 5898–5951.
[6] Y.A. Vlasov, N. Yao, D.J. Norris, Synthesis of photonic crystals for optical wavelengths from semiconductor quantum dots, Adv. Mat. 11 (1999) 165–169.
[7] P.C. Hiemenz, R. Rajagopalan. Principles of colloid and surface chemistry, 3rd edn, Dekker, New York, 1997.
[8] X. Zhou, L. Lei, Y. Zeng, X. Lu, F. Liang, L. Zhang, G. Lin, High salinity effects on the depletion attraction in colloid-polymer mixtures, J. Colloid Interface Sci. 631 (2023) 155–164.
[9] F. Sciortino, P. Tartaglia, Glassy colloidal systems, Adv. Phys. 54 (2005) 471–524.
[10] N. Willenbacher, J.S. Vesaratchanon, O. Thorwarth, E. Bartsch, An alternative route to highly concentrated, freely flowing colloidal dispersions, Soft Matter 7 (2011) 5777–5788.
[11] M. Wiemann, N. Willenbacher, E. Bartsch, Effects of cross-link density on re-entrant melting of microgel colloids. Colloids Surf. A: Physicochem. Eng. Asp. 413 (2012) 78–83.
[12] W. Hoover, F. Ree, Use of computer experiments to locate the melting transition and calculate the entropy in the solid phase, J. Chem. Phys. 47 (1967) 4873–4878.
[13] W. Wood, J. Jacobson, Preliminary results from a recalculation of the monte carlo equation of state of hard spheres, J. Chem. Phys. 27 (1957) 1207–1208.
[14] C. Weis, I. Natalia, N. Willenbacher, Effect of weak attractive interactions on flow behavior of highly concentrated crystalline suspensions, J. Rheol. 58 (5) (2014) 1583–1597.
[15] H. Lekkerkerker, W. Poon, P. Pusey, A. Stroobants, P. Warren, Phase behavior of colloid-polymer mixtures, Europhys. Lett. 20 (6) (1992) 559–564.
[16] R. Beyer, S. Iacopini, T. Palberg, H. Schöpe, Polymer induced changes of the crystallization scenario in suspensions of hard sphere like microgel particles, J. Chem. Phys. 136 (2012), 234906-234906.
[17] J. Bergenholtz, W. Poon, M. Fuchs, Gelation in model colloid-polymer mixtures, Langmuir 19 (2003) 4493–4503.
[18] Y. Chen, K. Schweizer, Microscopic theory of gelation and elasticity in polymer-particle suspensions, J. Chem. Phys. 120 (15) (2004) 7212–7222.
[19] G. Fritz, V. Schädler, N. Willenbacher, N.J. Wagner, Electrosteric stabiliztion of colloidal dispersions, Langmuir 18 (16) (2002) 6381–6390.
[20] J.L. Ortega-Venuesa, A. Martin-Rodriguez, R. Hidalgo-Alvarez, Colloidal stability of polymer colloids with different interfacial properties: mechanisms, J. Colloid Interface Sci. 184 (1996) 259–267.
[21] X. Guo, M. Ballauff, Spatial dimensions of colloidal polyelectrolyte brushes as determined by dynamic light scattering, Langmuir 16 (2000) 8719–8726.
[22] X. Guo, M. Ballauff, Spherical polyelectrolyte brushes: comparison between annealed and quenched brushes, Phys. Rev. E 64 (2001) 1–9, 051406.
[23] F.M. Horn, W. Richtering, J. Bergenholtz, N. Willenbacher, N.J. Wagner, Hydrodynamic and colloidal interactions in concentrated charge-stabilized polymer dispersions, J. Colloid Interface Sci. 225 (2000) 166–178.
[24] K.N. Pham, A.M. Puertas, J. Bergenholtz, S.U. Egelhaaf, A. Moussaïd, P.N. Pusey, A. B. Schofield, M.E. Cates, M. Fuchs, W.C.K. Poon, Multi-ple glassy states in a simple model system, Science 296 (2002) 104–106.
[25] T. Eckert, E. Bartsch, Reentrant glass transition in a colloid-polymer mixture with depletion attractions, Phys. Rev. Lett. 89 (2002) 1–4, 125701.
[26] U. Kumar, D. Ray, S. Abbas, D. Saha, V.K. Aswal, J. Kohlbrecher, Reentrant phase behavior of nanoparticle solutions probed by small-angle scattering, Curr. Opin. Colloid Interface Sci. 42 (2019) 17–32.
[27] L. Feng, B. Laderman, S. Sacanna, P. Chaikin, Re-entrant solidification in polymer–colloid mixtures as a consequence of competing entropic and enthalpic attractions. Nat. Mater. 14 (2015) 61–65.
[28] J.S. Vesaratchanon, K. Takamura, N. Willenbacher, Surface characterization of functionalized latexes with different surface functionalities using rheometry and dynamic light scattering, J. Colloid Inter. Sci. 345 (2010) 214–221.
[29] S. Maron, P. Pierce, Application of Ree-Eyring generalized flow theory to supensions of spherical particles, J. Colloid Sci. 11 (1956) 90–95.
[30] S. Asakura, F. Oosawa, Interaction between particles suspended in solutions of macromolecules, J. Polym. Sci. 33 (1958) 183–192.
[31] S. Kawaguchi, G. Imai, J. Suzuki, A. Miyahara, T. Kitano, K. Ito, Aqueous solution properties of oligo- and poly(ethylene oxide) by static light scattering and intrinsic viscosity, Polymer 38 (1997) 2885–2891.
[32] A. Kowalczyk, C. Oelschlaeger, N. Willenbacher, Visualization of microscale inhomogeneities in acrylic thickener solutions: a multiple particle tracking study, Polymer 58 (2015) 170–179.
[33] R. Bubeck, C. Bechinger, S. Neser, P. Leiderer, Melting and re-entrant freezing of two-dimensional colloidal crystals in confined geometry, Phys. Rev. Lett. 82 (1999) 3364–3367.
[34] S. Neser, C. Bechinger, P. Leiderer, T. Palberg, Finite size effects on the close packing of hard spheres, Phys. Rev. Lett. 79 (1997) 2348–2351.

[35] J.C. Crocker, D.G. Grier, Methods of digital video microscopy for colloidal studies, J. Colloid Interface Sci. 179 (1995) 298–310.
[36] D. Wirtz, Particle-tracking microrheology of living cells: principles and applications, Annu. Rev. Biophys. 38 (2009) 301–326.
[37] T.G. Mason, D.A. Weitz, Optical measurements of frequency-dependent linear viscoelastic moduli of complex fluids, Phys. Rev. Lett. 74 (7) (1995) 1250–1253.
[38] E.R. Weeks, J.C. Crocker, A.C. Levitt, A. Schofield, D.A. Weitz, Three-dimensional direct imaging of structural relaxation near the colloidal glass transition, Science 287 (5453) (2000) 627–631.
[39] C. Oelschlaeger, J. Marten, F. Péridont, N. Willenbacher, Imaging of the microstructure of Carbopol dispersions and correlation with their macroelasticity: a micro- and macrorheological study, J. Rheol. 66 (2022) 749–760.
[40] J. Mewis, N. Wagner, Colloidal suspension rheology, Cambridge University Press, 2011.
[41] S.M. Ilett, A. Orrock, W.C.K. Poon, P.N. Pusey, Phase behavior of a model colloid-polymer mixture, Phys. Rev. E 51 (1995) 1344–1352.